4836 *Inorg. Chem.* **2010**, *49*, 4836–4842
DOI: 10.1021/ic902079u

Inorganic Chemistry
Article

Hydrogenation Inducing Ferromagnetism in the Ternary Antiferromagnet NdCoSi

Sophie Tencé,[†,‡] Samir F. Matar,[†] Gilles André,[‡] Etienne Gaudin,[†] and Bernard Chevalier*[,†]

[†]*CNRS, Université de Bordeaux, ICMCB, 87 avenue du Docteur Albert Schweitzer, 33608 Pessac Cedex, France, and* [‡]*CEA, IRAMIS, LLB, 91191 Gif-sur-Yvette Cedex, France*

Received October 21, 2009

The hydride NdCoSiH obtained by exposure at 523 K of the ternary antiferromagnet NdCoSi under a pressure of 4 MPa of hydrogen crystallizes in the tetragonal ZrCuSiAs-type structure where H atoms occupy the tetrahedral [Nd_4] site. The hydrogenation induces an increase in the unit cell volume close to 6%. The investigation of NdCoSiH by magnetization measurements reveals its ferromagnetic behavior below $T_C = 20.5(5)$ K. Neutron powder diffraction shows that the T_C temperature is associated with a ferromagnetic arrangement of the Nd moments (2.3(2) μ_B at 1.5 K) parallel to the *c* axis as observed for NdFeSi. The magnetic properties, magnetic structure, and the value of the Nd ordered magnetic moment evidenced for NdCoSiH are discussed using both band structure calculations and a comparison with the behavior of NdCoSi and NdFeSi.

Introduction

Recently, it was reported that the ternary silicide CeCoSi crystallizing in the tetragonal CeFeSi-type structure absorbs hydrogen.[1−4] The resulting hydride CeCoSiH is stable under ambient conditions and adopts the tetragonal ZrCuSiAs-type structure, the H atoms being inserted in the [Ce_4] tetrahedral sites.[2] It is interesting to mention that the rare earth transition metal phosphide oxides RECoPO and REFePO (RE = Rare Earth) crystallize in a similar ZrCuSiAs-type structure where O atoms occupy [RE_4] tetrahedral sites[5] and some of them exhibit superconducting properties such as (La or Pr or Nd)FePO.[6,7]

The H-insertion into CeCoSi induces an increase of the unit cell volume and also the occurrence of an original transition from antiferromagnetic to spin fluctuation behavior.[1] In other words, the hydrogenation of CeCoSi involves a valence transition of cerium from trivalent to an intermediate valent state. The analysis of the electronic structures and of the chemical bonding properties of CeCoSi and its hydride, calculated in the framework of the local spin density approximation LSDA[8,9] to the density functional theory DFT,[10,11] reveals strong Ce−H interactions, which are bonding throughout the conduction band.[1] These Ce−H interactions are responsible for the valence transition observed for cerium in the sequence CeCoSi → CeCoSiH.[3]

Considering the results obtained on CeCoSiH, it is interesting to study the influence of the RE−H bonding on the magnetic properties of a similar hydride based on a normal rare earth element such as neodymium. Using magnetization measurements and neutron powder diffraction, Welter et al.[12] report that NdCoSi is an antiferromagnet below T_N = 7 K, and its magnetic structure consists of ferromagnetic (001) planes of Nd atoms with a coupling sequence (++−−) along the *c* axis. In other words, the Nd−Nd interaction is ferromagnetic inside the [Nd_4] tetrahedra and antiferromagnetic between two adjacent tetrahedra.

In this paper, we report on the synthesis of the hydride NdCoSiH and its investigation by X-ray and neutron powder diffraction and magnetization measurements. The magnetic sequence antiferromagnetic → ferromagnetic evidenced by hydrogenation of NdCoSi is discussed by considering the effects of the H insertion within the ternary silicide at the levels of the magneto-volume and chemical bonding with the help of computations within the well established density functional theoretical (DFT) framework.[10,11]

Experimental Section

Synthesis and Hydrogenation. Two polycrystalline NdCoSi samples of different mass (respectively 3 and 10 g) were synthesized by

*Author to whom correspondence should be addressed. E-mail: chevalie@icmcb-bordeaux.cnrs.fr.

(1) Chevalier, B.; Matar, S. F. *Phys. Rev. B* **2004**, *70*, 174408.
(2) Chevalier, B.; Pasturel, M.; Bobet, J.-L.; Isnard, O. *Solid State Commun.* **2005**, *134*, 529.
(3) Chevalier, B.; Matar, S. F.; Ménétrier, M.; Sanchez Marcos, J.; Rodriguez Fernandez, J. *J. Phys.: Condens. Matter* **2006**, *18*, 6045.
(4) Chevalier, B.; Matar, S. F.; Sanchez Marcos, J.; Rodriguez Fernandez, J. *Physica B* **2006**, *378−380*, 795.
(5) Zimmer, B. I.; Jeitschko, W.; Albering, J. H.; Glaum, R.; Reehuis, M. *J. Alloys Compd.* **1995**, *229*, 238.
(6) Kamihara, Y.; Hiramatsu, H.; Hirano, M.; Kawamura, R.; Yanagi, H.; Kamiya, T.; Hosono, H. *J. Am. Chem. Soc.* **2006**, *128*, 10012.
(7) Baumbach, R. E.; Hamlin, J. J.; Shu, L.; Zocco, D. A.; Crisosto, N. M.; Maple, M. B. *New J. Phys.* **2009**, *11*, 025018.
(8) von Barth, J.; Hedin, D. *J. Phys. C* **1972**, *5*, 1629.
(9) Janak, J. F. *Solid State Commun.* **1978**, *25*, 53.
(10) Kohn, W.; Sham, L. J. *Phys. Rev.* **1965**, *140A*, 1133.
(11) Hohenberg, P.; Kohn, W. *Phys. Rev.* **1964**, *136B*, 864.
(12) Welter, R.; Venturini, G.; Ressouche, E.; Malaman, B. *J. Alloys Compd.* **1994**, *210*, 279.

 Published on Web 04/29/2010

arc melting a stoichiometric mixture of pure elements (purity above 99.9%) in a high-purity argon atmosphere. Then, the samples were turned and remelted several times to ensure homogeneity. Annealing was done for one month at 1073 K by enclosing the samples in an evacuated quartz tube. Hydrogen absorption experiments were performed using the apparatus formerly described.[13] An annealed ingot was heated under a vacuum at 523 K for 12 h and then exposed to 4 MPa of hydrogen gas at the same temperature. The amount of absorbed H was determined volumetrically, using the sample having the smaller mass (3 g), by monitoring pressure changes in a calibrated volume. Under the experimental conditions described above, NdCoSi as CeCoSi[1] absorbs hydrogen. The amount of H atoms inserted is 1.0(1) per NdCoSi formula unit. The formed hydride is stable in the air.

X-Ray Powder Diffraction. X-ray powder diffraction with the use of a Philips 1050-diffractometer (Cu Kα radiation) was applied for the characterization of the structural type and for the phase identification of the ternary silicide samples before and after hydrogen absorption. The X-ray powder pattern of the sample having the smaller mass (3 g) is fully indexed on the basis of a tetragonal unit cell having the CeFeSi-type structure. No parasitic phase is detected. The unit cell parameters deduced from this investigation, $a = 4.027$ and $c = 6.897$ Å, agree with those reported previously.[12] On the contrary, some amounts of $NdCo_2Si_2$ are present as an impurity phase in the sample having the higher mass (10 g). This sample, after hydrogenation, is used for neutron powder diffraction. It was checked that $NdCo_2Si_2$ does not absorb hydrogen at 523 K and at least up to 4 MPa.

The crystal structure of the hydride NdCoSiH adopts the same space group type ($P4/nmm$) as the initial ternary silicide NdCoSi, but the hydrogenation causes a pronounced anisotropic expansion of the unit cell; the a parameter decreases from 4.027 to 3.927 Å (−2.5%), whereas the c parameter increases strongly from 6.897 to 7.695 Å (+11.6%). In other words, H-insertion into NdCoSi involves an expansion of the unit cell volume from 111.85 to 118.67 Å^3 (+6.1%). These structural characteristics are comparable to those reported during the hydrogenation of the CeCoSi ternary silicide.[1]

Magnetization Measurements. For these measurements, the NdCoSiH sample was compacted at room temperature (ca. 80% compactness) to a pellet of 6 mm diameter and 3 mm thickness. The latter was heated for two days at 523 K under a pressure of 4 MPa hydrogen; this pellet, checked by X-ray diffraction, reveals a random orientation of the grains. Magnetization measurements were performed on a part of the pellet using a Superconducting Quantum Interference Device (SQUID) magnetometer in the temperature range 1.8−300 K and applied fields up to 4.8 T. Finally, a small piece of the initial NdCoSi ingot was used for these measurements.

Neutron Powder Diffraction. This investigation was performed at the Orphée reactor (CEA/Saclay, France) on the two-axis diffractometer G4.1 ($\lambda = 2.423$ Å; 800 cell-position-sensitive detector) and 3T2 ($\lambda = 1.2262$ Å; high resolution powder diffractometer). The data were analyzed using the Rietveld profile method by means of the Fullprof program,[14] with neutron scattering lengths and magnetic form factors of Nd taken respectively from refs 15 and 16.

Computational Details. Calculations are all-electron on the basis of the density functional theory (DFT) framework as built within the scalar relativistic (spin-only moments) augmented spherical wave (ASW) method in its full potential implementation.[17,18] Effects of exchange and correlation were accounted for with the Wu et al. GGA scheme.[19] The wave function is expanded in atom-centered augmented spherical waves, which are Hankel functions and numerical solutions of Schrödinger's equation, respectively, outside and inside the so-called augmentation spheres. All valence electrons, including 4f(Nd) were treated as band states. We shall further discuss this point in the density of states section.

In the minimal ASW basis set, we chose the outermost shells to represent the valence states, and the matrix elements were constructed using partial waves up to $l_{max} + 1 = 4$ for Nd, $l_{max} + 1 = 3$ for Co, $l_{max} + 1 = 2$ for Si, and $l_{max} + 1 = 1$ for H. Considering the 4f(Nd) states within the valence basis set does not mean they are taken as totally itinerant in as far as spin polarization due to 4f is of intraband nature while the itinerant part of the Nd valence basis set contributes to the bonding within NdCoSi and its hydride. The completeness of the valence basis set—without calling for semi core states—was checked for charge convergence with an $l_{max} + 1$ occupation less than 0.1 electrons. Regarding the angular momentum expansions, they are in principle carried to infinity. The self-consistent field calculations are run to a charge convergence of $\Delta Q \sim 10^{-8}$ and the accuracy of the method is in the range of about 0.1 to 1 meV regarding energy differences. A sufficiently large number of k points were used to sample the irreducible wedge of the tetragonal Brillouin zone (i.e., from 6 6 6 up to 14 14 14 k_x, k_y, k_z).

All calculations start from neutral atoms with enforced spin degeneracy pertaining to a nonmagnetic configuration (NM). Due to their construction based on an electron gas, the usual DFT functional (LDA and GGA) cannot correctly account for the regular neodymium magnetic moments due to the localization of the 4f states. For this reason, we present tentative magnitudes of the moments in spin polarized calculations (SP).

Besides the atom-resolved electronic structure, with the total and site projected density of states (PDOS), the chemical interaction between the atoms is discussed using the overlap (S_{ij}) within the COOP (Crystal Orbital Overlap Population) criterion.[20] Further, a mapping of the electrons within the lattice will be provided within the electron localization function (ELF) scheme.[21] It allows a determination of the amount of localization of electrons with respect to the free electron gas distribution. The dimensionless ELF magnitude ranges from 0 to 1 with ELF = 1/2 corresponding to the free electron gas distribution. These three extreme situations will be illustrated by three sets of colors: ELF = 0 points to no localization (blue contours), ELF = 1 indicates strong localization (red contours), and ELF = 1/2 (green contours) is expected for metallic systems. We have successfully used this computational scheme for similar the isotypic silicide CeCoSi.[1]

Results and Discussion

Magnetic Properties. Figure 1 presents, at low temperatures, the dependence of the magnetization M for NdCoSi and its hydride. For an applied field of $\mu_0 H = 0.1$ T, the curve M versus T of NdCoSi (inset of Figure 1) exhibits a sharp maximum at $T_N = 7.5(5)$ K, suggesting an antiferromagnetic ordering as reported previously.[12] The value of the Néel temperature T_N is close to that determined (7(1) K) by Welter et al.[12] On the contrary, for the hydride NdCoSiH, the strong increase of M versus T characterizes the occurrence of a ferromagnetic ordering. The Curie temperature T_C, was determined from the inflection point of the curve M versus T is 20.5(5) K. Above 75 K, the reciprocal magnetic susceptibility χ_m^{-1} of NdCoSiH

(13) Bobet, J.-L.; Pechev, S.; Chevalier, B.; Darriet, B. *J. Alloys Compd.* **1998**, *267*, 136.
(14) Rodriguez-Carvajal, J. Satellite Mtg 15th Congr. IUCr on Powder Diffraction, Toulouse, France, **1990**; p 127.
(15) Sears, V. F. *Neutron News* **1992**, *3*, 26.
(16) Freeman, A. J.; Desclaux, J. P. *J. Magn. Magn. Mater.* **1979**, *12*, 11.
(17) Williams, A. R.; Kübler, J.; Gelatt, C. D. *Phys. Rev. B* **1979**, *19*, 6094.
(18) Eyert, V. *The Augmented Spherical Wave Method - A Comprehensive Treatment, Lect. Notes Phys. 719*; Springer: Berlin, 2007.
(19) Wu, Z.; Cohen, R. E. *Phys. Rev. B* **2006**, *73*, 235116.
(20) Hoffmann, R. *Angew. Chem., Int. Ed. Engl.* **1987**, *26*, 846.
(21) Becke, A. D.; Edgecombe, K. E. *J. Chem. Phys.* **1990**, *92*, 5397.

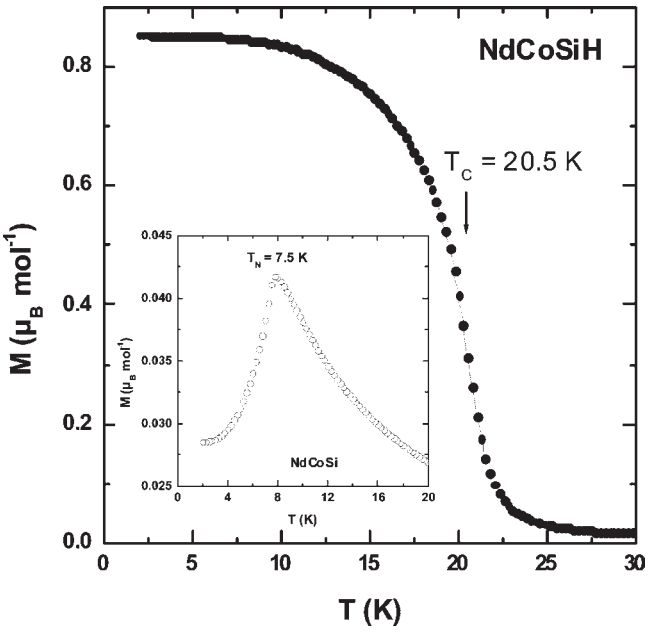

Figure 1. Temperature dependence of the magnetization, measured with an applied field μ_0H = 0.1 T, for NdCoSi (inset) and its hydride NdCoSiH.

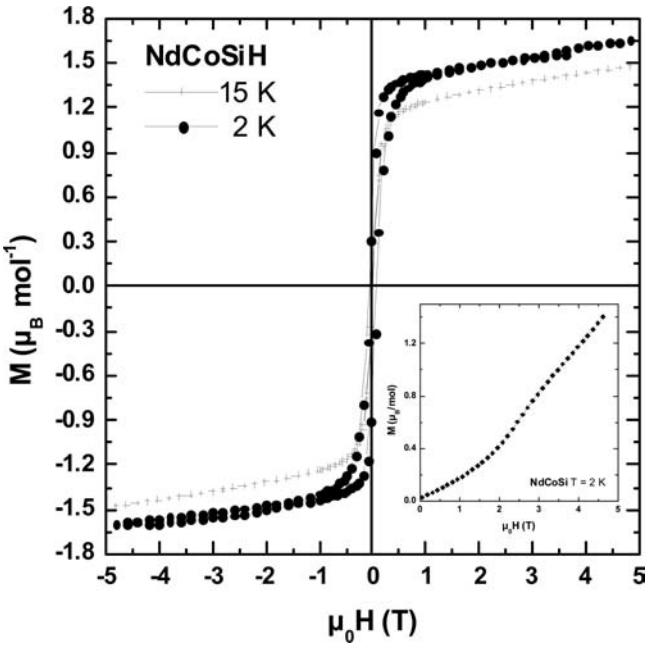

Figure 2. Field dependence at 2 and 15 K of the magnetization M for NdCoSiH. The inset presents the curve M versus μ_0H for NdCoSi cooled at 2 K.

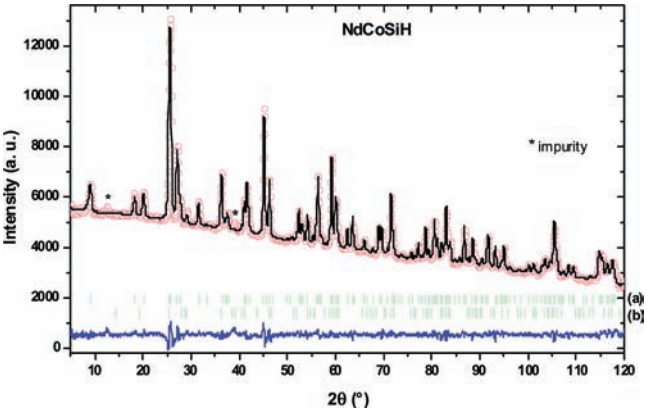

Figure 3. Rietveld profile refinement for NdCoSiH at 300 K (λ = 1.2262 Å). The open circles represent the observed data points; the solid lines reveal the calculated profile and the difference (bottom) between the observed and calculated profiles. The tics correspond to 2θ-Bragg positions for NdCoSiH (a) and $NdCo_2Si_2$ (b).

measured with an applied field of 4 T (not shown here) follows a Curie−Weiss law. The experimental value of the effective magnetic moment μ_{eff} = 3.69(5) μ_B/Nd is close to the calculated value for a free Nd^{3+} ion (3.62 μ_B/Nd). This experimental μ_{eff} value, which is lower than that reported for NdCoSi (3.9 μ_B),[12] suggests that Co is nonmagnetic in the hydride. The paramagnetic Curie temperature θ_p was found to be −7.0(5) K. Such a negative value of θ_p is sometimes observed for neodymium-based ferromagnets such as $NdOs_4Sb_{12}$;[22] this behavior is linked to the influence of the crystalline electric field (CEF) on the ground state of the Nd^{3+} ion.

Below T_C, the hysteresis curves for NdCoSiH (Figure 2) agree with the behavior of a polycrystalline ferromagnet. The loop exhibits a very small coercive field of 0.07 T at 2 K and the magnetization M is not saturated at 4.8 T, reaching a value of 1.65(5) μ_B/Nd. This value of M, notably smaller than that expected for a Nd^{3+} magnetic moment (3.27 μ_B/Nd), results from the mean powder average of the sample (random distribution of grains). Finally, we mention that the curve M versus μ_0H measured at 2 K (inset of Figure 2) shows that NdCoSi is a metamagnet; M, as μ_0H increases, varies linearly for μ_0H < 1.5 T and then increases more rapidly.

Crystal and Magnetic Structures. The neutron diffraction pattern collected at 300 K using the 3T2 diffractometer for NdCoSiH (Figure 3) reveals the presence of $NdCo_2Si_2$ (~8 wt %) and an unknown phase as an impurity (less than 5 wt %). *The high background value is due to the high incoherent scattering cross-section of hydrogen*. This pattern shows that the hydride adopts the tetragonal ZrCuSiAs-type structure; the results of the refinement of the crystal structure of NdCoSiH are given in Table 1. The absorption correction has been taken into account in the refinement with respect to the sample nature, the holding geometry, and the used wavelength (μR = 0.45).

Table 1. Lattice, Positional, and Isotropic Displacement Parameters at 300 K for NdCoSiH (space group $P4/nmm$)[a]

			positional parameters			
atom	site[b]	occ.	x	y	z	B_{ISO} (Å^2)
Nd	2c	1	1/4	1/4	0.6710(2)	0.53(2)
Co	2a	1	3/4	1/4	0	0.64(6)
Si	2c	1	1/4	1/4	0.1554(4)	0.80(4)
H	2b	0.95(1)	1/4	3/4	1/2	1.77(8)

[a] The reliability factors are R_p = 14.9%, R_{wp} = 12.8%, and R_B = 5.6%. [b] a = 3.9279(1) and c = 7.6935(4) Å.

The refinement confirms the results obtained by X-ray powder diffraction and shows (i) that the H-insertion into

(22) Ho, P. C.; Yuhasz, W. M.; Butch, N. P.; Frederick, N. A.; Sayles, T. A.; Jeffries, J. R.; Maple, M. B.; Betts, J. B.; Lacerda, A. H.; Rogl, P.; Giester, G. *Phys. Rev. B* **2005**, *72*, 094410.

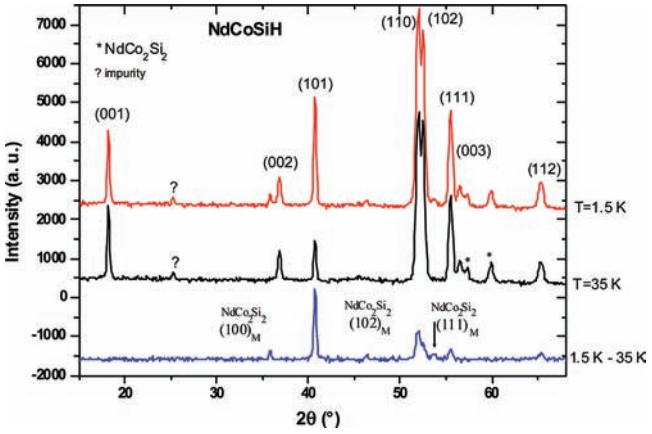

Figure 4. Neutron diffraction patterns for NdCoSiH at 35 and 1.5 K, as well as the difference pattern "1.5−35 K" (λ = 2.423 Å). The nuclear (∗) and the magnetic (M) reflections of the $NdCo_2Si_2$ impurity are indicated as well as that of the nonidentified impurity.

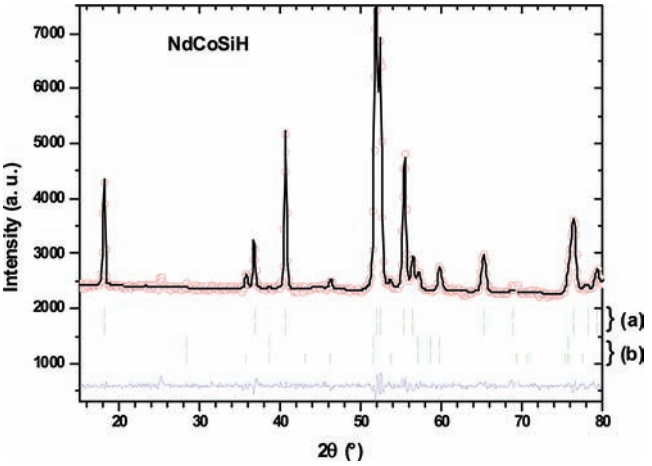

Figure 5. Rietveld profile refinement of the pattern at 1.5 K for NdCoSiH (λ = 2.423 Å). The ticks correspond to nuclear and magnetic 2θ-Bragg positions for NdCoSiH (a) and $NdCo_2Si_2$ (b).

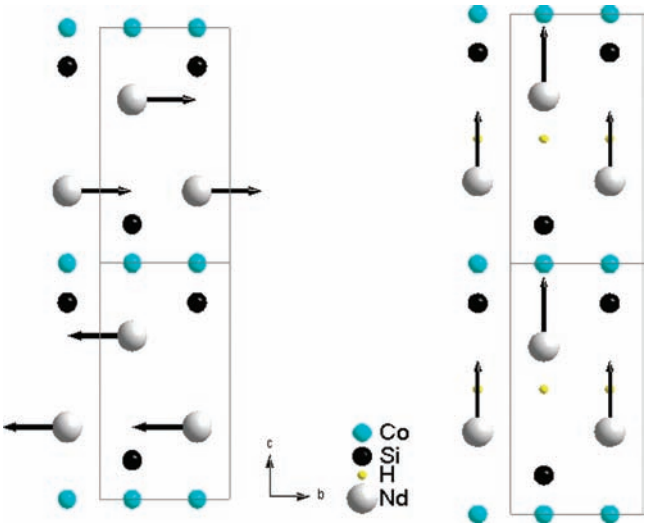

Figure 6. Magnetic structures for NdCoSi (left) and NdCoSiH (right) in projection along the *a* axis.

NdCoSi induces an anisotropic expansion of the unit cell since the *a* parameter decreases whereas the *c* parameter increases, (ii) an increase of the unit cell volume during the hydrogenation, and (iii) that the [Nd_4] site devoted to hydrogen is almost fully occupied; the calculated occupancy 0.95(1) agrees with the value determined volumetrically by the hydrogen absorption experiment (1.0(1)). The refinement of the reflections' profiles allows us to obtain the size of the coherent domains. We find an isotropic correlation length of 318(5) Å, which is quite low. This can be due to structural defects induced by hydrogen insertion; this hypothesis could be verified by neutron diffraction investigation performed on analogous deuteride.

Neutron powder diffraction patterns were recorded between 35 and 1.5 K on the two-axis diffractometer G4.1 (Figure 4). At 35 K, the peaks are only of nuclear origin, and the refinement of the intensities is in good agreement with that obtained with the high resolution spectrometer data (3T2 diffractometer). This pattern reveals also some peaks attributed to the $NdCo_2Si_2$ impurity phase; the nuclear and magnetic structures of this last ternary silicide were reported previously in ref 23. Indeed, the reflections corresponding to NdCoSiH and $NdCo_2Si_2$ are separated enough to consider that the refinement of the hydride nuclear structure is almost independent of the nuclear structure of $NdCo_2Si_2$. The pattern at 1.5 K, below the ferromagnetic transition, shows no additional reflections with respect to the nuclear data but an increase in the intensity of some nuclear reflections. The propagation vector associated with the magnetic structure is thus k = (0 0 0), which corresponds to the ferromagnetic order. The absence of magnetic contribution to the (001) reflection suggests that the Nd magnetic moments are aligned along the *c* axis. The best refinement ($R_{B\text{-nucl}}$ = 2.4% and $R_{B\text{-mag}}$ = 2.2%) is actually obtained with a ferromagnetic model where the Nd moments are parallel to the *c* axis (Figure 5). The Nd moment value amounts to 2.3(2) μ_B at 1.5 K, which is weakly higher than the value deduced from the magnetization measurements (1.65(5) μ_B at 2 K; Figure 2); this last average value results from the statistical distribution of the ferromagnetic grains. Finally, the Nd moment determined by neutron powder diffraction is lower than the theoretical one expected for the Nd^{3+} free ion (3.27 μ_B) but comparable to that determined for NdCoSi (2.08 μ_B)[12] and NdFeSi (2.58(8) μ_B).[24] This reduction may be explained by the influence of the crystalline electric field effect as reported for the last ternary silicides.

The ferromagnetic structure of NdCoSiH is compared to that of the initial antiferromagnet NdCoSi in Figure 6. For NdCoSiH, the magnetic structure corresponds to a stacking of (001) ferromagnetic sheets, with Nd moments perpendicular to the sheets. This structure is similar to that reported for NdFeSi.[24] Also, in NdCoSi, the magnetic structure consists of (001) ferromagnetic planes of Nd moments with the coupling sequence (+ + − −) along the *c* axis, with Nd moments lying into the basal plane. In other words, in the sequence NdCoSi → NdCoSiH, the hydrogenation (i) induces a change of the direction of the

(23) Shigeoka, T.; Iwata, N.; Hashimoto, Y.; Andoh, Y.; Fujii, H. *J. Phys.* (*Paris*) **1988**, *49*, C8–431.

(24) Welter, R.; Venturini, G.; Malaman, B. *J. Alloys Compd.* **1992**, *189*, 49.

Nd moments from perpendicular to parallel to the c axis and (ii) produces positive coupling between all the (001) ferromagnetic layers.

Finally, the temperature dependence of the Nd magnetic moment value (not shown here), deduced from the different patterns below 35 K, vanishes around 20.7(5) K, which is in fair agreement with the Curie temperature T_C deduced from the magnetization measurements.

Electronic Structure Calculations. The spin polarized (SP) calculations are done by allowing for two spin occupations (↑ and ↓). Then, the resulting magnetic moments and energy differences between the ferromagnetic SP (SP-Ferro) and antiferromagnetic SP (SP-Anti Ferro) can be analyzed.

Discussing first the magnitudes of the magnetic polarization, in the SP-Ferro configuration, the Nd magnetic moment decreases slightly from NdCoSi (3.3 μ_B) to NdCoSiH (3.2 μ_B). While the Nd−H interaction could contribute to the slight lowering of the magnetic moment magnitude, it seems more likely to assign a relatively constant Nd moment mainly governed by CEF effects. The ordered magnetic moment development is partly (itinerant electrons) mediated by the electron gas, and the Co 3d band polarization leads to a small magnitude moment of ~0.03 μ_B, therefore, merely exchange-induced. When the SP-Anti Ferro configuration is accounted for within NdCoSi, the calculations yield a lower energy with ΔE(SP-Anti Ferro − SP-Ferro) = −1.74 eV/fu so that the SP-Anti Ferro ground state is confirmed for NdCoSi in agreement with the experiment. The absolute value of the Nd moment decreases (3.1 μ_B), due to symmetry breaking when half of the constituents are counted as UP-spin and the other half as DOWN-spin. When H is introduced, the magnetic moment decreases in absolute value (3.2 μ_B) but remains larger than in NdCoSi SP-Anti Ferro. As expected, Si and H carry very small moments which arise from the quantum mixing of their valence states with the Nd/Co magnetic ones. Our presentation of the magnitudes of moments is proposed at a qualitative level due to the weaknesses of the exchange correlation functional used in the calculations.

Figure 7 shows the site and spin projected density of states (PDOS) for SP-Ferro of NdCoSi, NdCoSiH, and NdCoSi expanded (in order to represent the correct shape of the crystal potential in the hydrogen free NdCoSiH, which we study to assess magneto-volume effects, additional augmentation spheres called empty spheres (ES, zero atomic number) were inserted at H positions). In this plot, as well as in the following ones, the zero energy (x axis) is with respect to the Fermi level E_F. At E_F, the major feature is the crossing at a large intensity of the 4f(Nd) states for majority spins (↑). The 4f (↓) band is within the conduction band at ~2 eV above. This is the magnitude of exchange splitting leading to the onset of the Nd magnetic moment. It is known that the LDA/GGA calculations lead to position the 4f band at the Fermi level erroneously. Then, the effect of the addition of the Hubbard repulsive U parameter is to force the occupied 4f states down in energy, within or well below the valence band of states. In the latter case, caused by large magnitudes of U (~ 6 eV), the 4f states become extremely narrow, indicating a lack of hybridization. For NdCoSi SP-Ferro (Figure 7a), we show such an effect on the 4f(Nd) sub-band with a value of U = 6.5 eV. The inset shows that the occupied 4f states are now at −6 eV (all ↑ spin polarized) within the valence band while the band of unoccupied 4f states is raised above the Fermi energy.

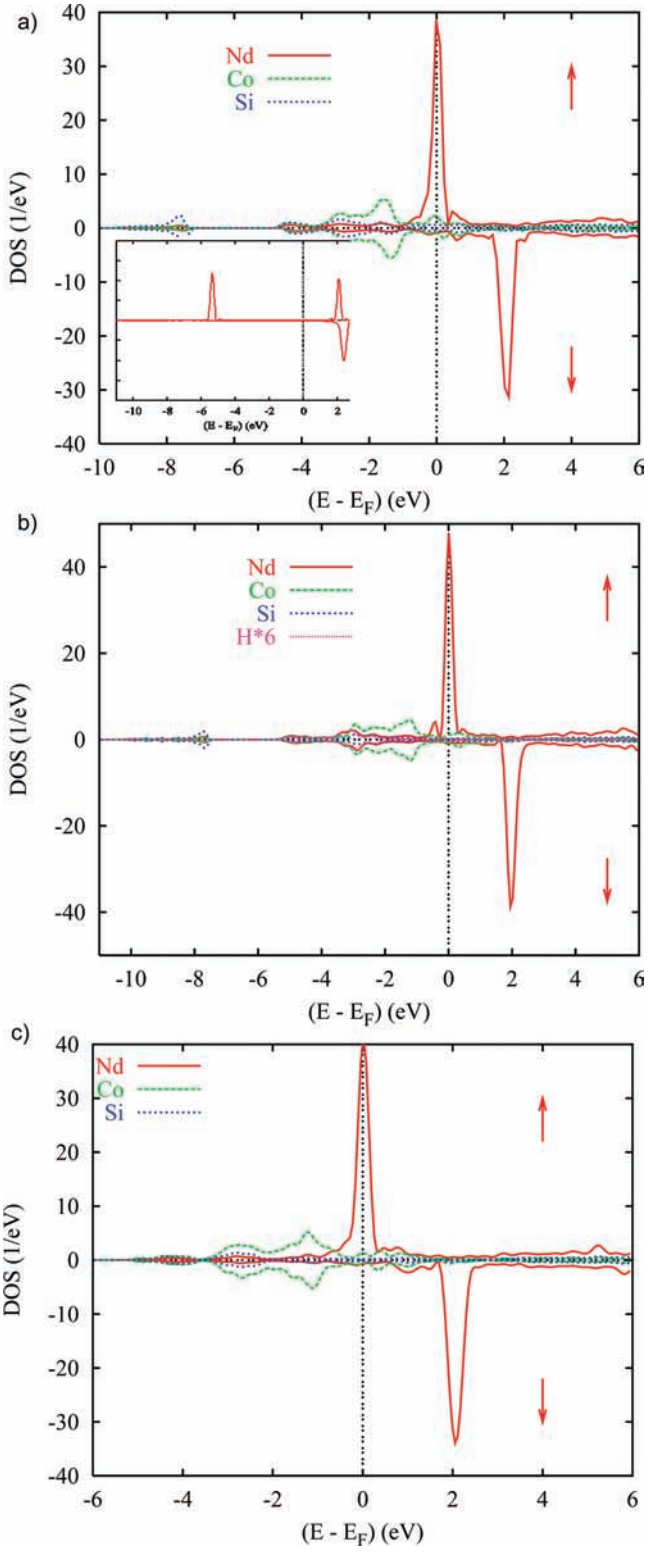

Figure 7. Site and spin projected density of states (PDOS) for a ferromagnetic configuration of (a) NdCoSi (the inset shows the change of Nd PDOS from GGA+U calculations), (b) NdCoSiH (H PDOS were artificially multiplied by 6 for sake of clear presentation), and (c) NdCoSi expanded.

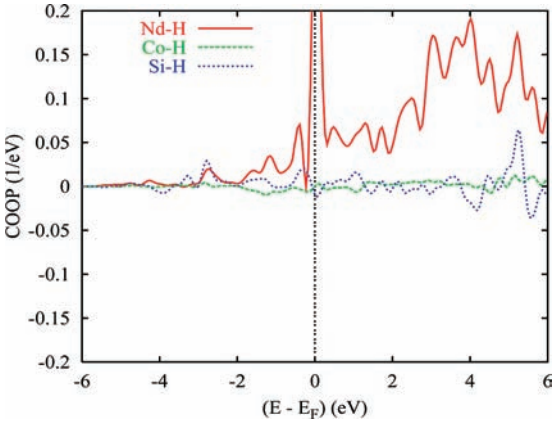

Figure 8. Chemical bonding with the COOP criterion for hydrogen bonding within NdCoSiH.

This picture is, however, more predominant in rare earth oxide systems such as $(RE)_2O_3$.[25] As a matter of fact, within the valence band (VB), there is a non-negligible contribution from Nd itinerant states below E_F which is responsible for the chemical bonding with other constituents. Due to the large filling of their 3d states, the Co (dashed, green line) PDOS are found within the VB around −2 eV. Spin polarization is seen to affect the Co d states within NdCoSi by shifting the majority spin (↑) states down in energy and the minority ones (↓) to higher energy. This is contrary to NdCoSiH SP-Ferro (Figure 7b) or to the expanded NdCoSi compound (Figure 7c), where there is hardly any energy shift. This can be assigned to distance changes between the major magnetic moment carrier (Nd) and the transition metal (Co): $d_{Nd-Co} = 2.93$ Å in NdCoSi and $d_{Nd-Co} = 3.20$ Å in the hydride (as well as within the expanded system). Low magnitude Si s and p-like states are observed throughout the VB; they show similar peak shapes not only for Co but for Nd as well. This indicates the hybridization between them. When H is introduced, the VB has extra states that are added through the redistribution of H s states over the available valence basis sets of neighboring atoms. Their quantum mixing is better shown from the chemical bonding discussion.

Figure 8 illustrates the bonding characteristics in NdCoSiH (NM configuration) based on the crystal orbital overlap population (COOP) introduced above in the Computational Details section. Along the *y* axis, positive, negative, and zero COOP correspond to bonding, antibonding, and nonbonding interactions, respectively. Clearly, the strongest bonding is for Nd−H due to the shortest interatomic distance ($d_{Nd-H} = 2.36$ Å) within the hydride structure, before it can be seen to involve not only itinerant states of Nd within the VB but 4f states at the Fermi level as well. Then, the spin pairing between Nd and H can affect the slight lowering of the moment carried by Nd; however, CEF effects should prevail.

The binding of hydrogen within the structure is expressed as follows for one formula unit (fu): $E_{stabil\ H} = 1/2\{E(NdCoSiH) - E(NdCoSi) - E(H_2)\}$. E(NdCoSiH) and E(NdCoSi) represent the total energies of the hydride and the ternary silicide, respectively. $E(H_2)$ is the energy of the dihydrogen molecule, which is computed by considering a cubic supercell. The obtained $E_{stabil.H}$ magnitude is then −0.92 eV, leading to confirmation of the effective chemical binding of H within the structure. In order to estimate the charge transfer onto H, a Bader charge analysis[26] for all constituents was subsequently carried out. As is expected in such an intermetallic compound, there is charge redistribution with a slight transfer from Nd and Co to Si (4.4 instead of 4 electron) and H (1.7 instead of 1 electron). This also agrees with the larger electronegativity of Si and H versus Nd and Co.

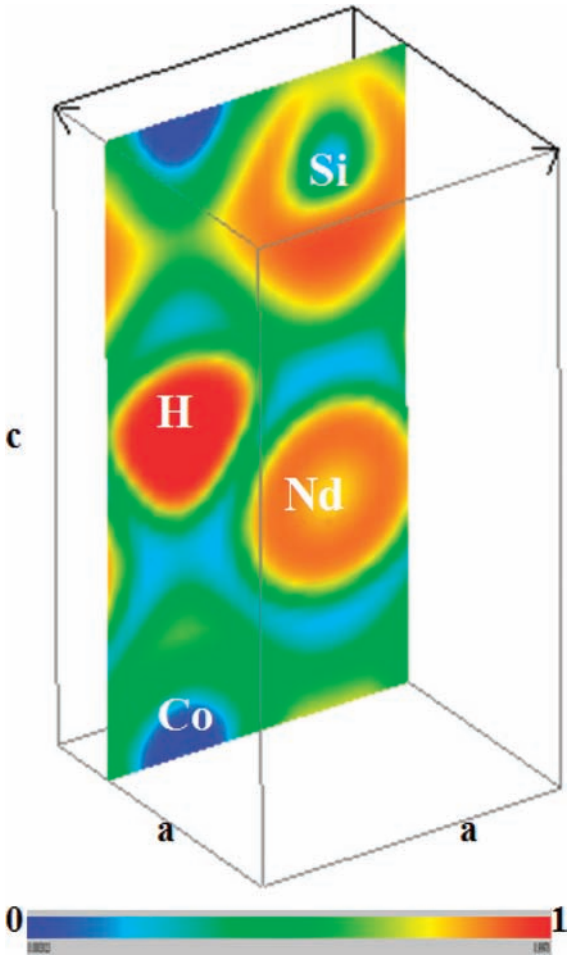

Figure 9. Electron localization function map for NdCoSiH showing a vertical plane containing all species. As indicated by the ruler at the bottom of the figure, red, green, and blue contours are for strong (ELF = 1), free-electron like, and no localization (ELF = 0), respectively.

Finally, we present the calculated electron localization function ELF map for a vertical plane including all atomic species (Figure 9). The actual localization is observed around hydrogen and silicon, while zero localization around cobalt can be observed. The hydrogen ELF contours are seen to distort toward Nd (orange contours due to 4f states within valence basis set), while those of Si tend toward Co. This is in accordance with the relatively short Co−Si distance of 2.27 Å, underlining the covalent Co−Si and Nd−H bonding.

(25) Skorodumova, N. V.; Ahuja, R.; Simak, S. I.; Abrikosov, I. A.; Johansson, B.; Lundqvist, B. I. *Phys Rev. B* **2001**, *64*, 115108.

(26) Bader, R. F. W. *Atoms in Molecules - A Quantum Theory*; Oxford University Press: Oxford, U. K., 1990.

The strong localization around hydrogen suggests the presence of negatively charged H ions in NdCoSiH as described in the Bader charge analysis above; in other words, the hydrogen takes one electron out of the conduction band. Thus, NdCoSiH and the ferromagnet NdFeSi possess the same number of conduction electrons. As the indirect RKKY magnetic interactions governing the magnetic properties of the rare earth based compounds are dependent both on the number of conduction electrons and on the rare earth-rare earth interatomic distances, NdCoSiH and NdFeSi exhibit consequently the same magnetic ordering. These ferromagnetic compounds present (i) a similar magnetic structure, (ii) a comparable Curie temperature, respectively 20.5 and 25 K for NdCoSiH and NdFeSi,[24] (iii) close values of the Nd moment, 2.3(2) μ_B for NdCoSiH and 2.58 μ_B for NdFeSi, and finally (iv) comparable shortest d_{Nd-Nd} distances of 3.825 and 3.779 Å for NdCoSiH and NdFeSi, respectively.[24]

Conclusion

Hydrogenation of the ternary compounds crystallizing in the tetragonal CeFeSi-type is an interesting route in order to modify their magnetic properties. It is shown here that the hydrogen insertion into NdCoSi induces a transition from antiferromagnetism to ferromagnetism. The hydride NdCoSiH exhibits magnetic properties very close to those reported for the ferromagnet NdFeSi. These behaviors were supported by DFT-based computations of NdCoSi and NdCoSiH in different magnetic configurations. A meaningful chemical role is found to be played by hydrogen in its interaction with neodymium.

Acknowledgment. The authors would like to thank R. Decourt for his assistance during the specific heat measurements. Computations were carried out on the mainframe supercomputers of the M3PEC-Mésocentre (MCIA- University Bordeaux 1), partly financed by the Conseil Régional d'Aquitaine, the French Ministry of research and technology, and the Institut des Grilles (CNRS). The authors are indebted to the Conseil Régional d'Aquitaine for financial support, especially S.T. for a Ph.D. stipend. Finally, B.C. thanks the European Science Foundation (ECOM-COST action P16) for financial support.